

GILE: A Generalized Input-Label Embedding for Text Classification

Nikolaos Pappas James Henderson

Idiap Research Institute, Martigny 1920, Switzerland

{nikolaos.pappas, james.henderson@idiap.ch}

Abstract

Neural text classification models typically treat output labels as categorical variables which lack description and semantics. This forces their parametrization to be dependent on the label set size, and, hence, they are unable to scale to large label sets and generalize to unseen ones. Existing joint input-label text models overcome these issues by exploiting label descriptions, but they are unable to capture complex label relationships, have rigid parametrization, and their gains on unseen labels happen often at the expense of weak performance on the labels seen during training. In this paper, we propose a new input-label model which generalizes over previous such models, addresses their limitations, and does not compromise performance on seen labels. The model consists of a joint non-linear input-label embedding with controllable capacity and a joint-space-dependent classification unit which is trained with cross-entropy loss to optimize classification performance. We evaluate models on full-resource and low- or zero-resource text classification of multilingual news and biomedical text with a large label set. Our model outperforms monolingual and multilingual models which do not leverage label semantics and previous joint input-label space models in both scenarios.

1 Introduction

Text classification is a fundamental NLP task with numerous real-world applications such as topic recognition (Tang et al., 2015; Yang et al., 2016), sentiment analysis (Pang and Lee, 2005; Yang et al., 2016), and question answering (Chen et al., 2015; Kumar et al., 2015). Classification also appears as a sub task for sequence prediction tasks such as neural machine translation (Cho et al., 2014; Luong et al., 2015), and summarization

(Rush et al., 2015). Despite the numerous studies, existing models are trained on a fixed label set using k-hot vectors and, therefore, treat target labels as mere atomic symbols without any particular structure to the space of labels, ignoring potential linguistic knowledge about the words used to describe the output labels. Given that semantic representations of words have been shown to be useful for representing the input, it is reasonable to expect that they are going to be useful for representing the labels as well.

Previous work has leveraged knowledge from the label texts through a joint input-label space, initially for image classification (Weston et al., 2011; Mensink et al., 2012; Frome et al., 2013; Socher et al., 2013). Such models generalize to labels both seen and unseen during training, and scale well on very large label sets. However, as we explain in Section 2, existing input-label models for text (Yazdani and Henderson, 2015; Nam et al., 2016) have the following limitations: (i) their embedding does not capture complex label relationships due to its bilinear form, (ii) their output layer parametrization is rigid because it depends on the dimensionality of the encoded text and labels, and, (iii) they are outperformed on seen labels by classification baselines trained with cross-entropy loss (Frome et al., 2013; Socher et al., 2013).

In this paper, we propose a new joint input-label model which generalizes over previous such models, addresses their limitations, and does not compromise performance on seen labels (see Figure 1). The proposed model is comprised of a joint non-linear input-label embedding with controllable capacity and a joint-space-dependent classification unit which is trained with cross-entropy loss to optimize classification performance.¹ The need for capturing complex label relationships is addressed by two non-linear transformations which have the same target joint space dimension-

¹Our code is available at: github.com/idiap/gile

ality. The parametrization of the output layer is not constrained by the dimensionality of the input or label encoding, but is instead flexible with a capacity which can be easily controlled by choosing the dimensionality of the joint space. Training is performed with cross-entropy loss, which is a suitable surrogate loss for classification problems, as opposed to a ranking loss such as WARP loss (Weston et al., 2010) which is more suitable for ranking problems.

Evaluation is performed on full-resource and low- or zero-resource scenarios of two text classification tasks, namely on biomedical semantic indexing (Nam et al., 2016) and on multilingual news classification (Pappas and Popescu-Belis, 2017) against several competitive baselines. In both scenarios, we provide a comprehensive ablation analysis which highlights the importance of each model component and the difference with previous embedding formulations when using the same type of architecture and loss function.

Our main contributions are the following:

- (i) We identify key theoretical and practical limitations of existing joint input-label models.
- (ii) We propose a novel joint input-label embedding with flexible parametrization which generalizes over the previous such models and addresses their limitations.
- (iii) We provide empirical evidence of the superiority of our model over monolingual and multilingual models which ignore label semantics, and over previous joint input-label models on both seen and unseen labels.

The remainder of this paper is organized as follows. Section 2 provides background knowledge and explains limitations of existing models. Section 3 describes the model components, training and relation to previous formulations. Section 4 describes our evaluation results and analysis, while Section 5 provides an overview of previous work and Section 6 concludes the paper and provides future research directions.

2 Background: Neural Text Classification

We are given a collection $D = \{(x_i, y_i), i = 1, \dots, N\}$ made of N documents, where each document x_i is associated with labels $y_i = \{y_{ij} \in \{0, 1\} \mid j = 1, \dots, k\}$, and k is the

total number of labels. Each document $x_i = \{w_{i1}, w_{i2}, \dots, w_{K_i T_{K_i}}\}$ is a sequence of words grouped into sentences, with K_i being the number of sentences in document i and T_j being the number of words in sentence j . Each label j has a textual description comprised of multiple words, $c_j = \{c_{j1}, c_{j2}, \dots, c_{jL_j} \mid j = 1, \dots, k\}$ with L_j being the number of words in each description. Given the input texts and their associated labels *seen* during the training portion of D , our goal is to learn a text classifier which is able to predict labels **both** in the seen, \mathcal{Y}_s , or unseen, \mathcal{Y}_u , label sets, defined as the sets of unique labels which have been seen or not during training respectively and, hence, $\mathcal{Y} \cap \mathcal{Y}_u = \emptyset$ and $\mathcal{Y} = \mathcal{Y}_s \cup \mathcal{Y}_u$.²

2.1 Input Text Representation

To encode the input text, we focus on hierarchical attention networks (HANs), which are competitive for monolingual (Yang et al., 2016) and multilingual text classification (Pappas and Popescu-Belis, 2017). The model takes as input a document x and outputs a document vector h . The input words and label words are represented by vectors in \mathbb{R}^d from the same³ embeddings $E \in \mathbb{R}^{|\mathcal{V}| \times d}$, where \mathcal{V} is the vocabulary and d is the embedding dimension; E can be pre-trained or learned jointly with the rest of the model. The model has two levels of abstraction, word and sentence. The word level is made of an encoder network g_w and an attention network a_w , while the sentence level similarly includes an encoder and an attention network.

Encoders. The function g_w encodes the sequence of input words $\{w_{it} \mid t = 1, \dots, T_i\}$ for each sentence i of the document, noted as:

$$h_w^{(it)} = g_w(w_{it}), t \in [1, T_i], \quad (1)$$

and at the sentence level, after combining the intermediate word vectors $\{h_w^{(it)} \mid t = 1, \dots, T_i\}$ to a sentence vector $s_i \in \mathbb{R}^{d_w}$ (see below), where d_w is the dimension of the word encoder, the function g_s encodes the sequence of sentence vectors $\{s_i \mid i = 1, \dots, K\}$, noted as $h_s^{(i)}$. The g_w and g_s functions can be any feed-forward (DENSE) or recurrent networks, e.g. GRU (Cho et al., 2014).

Attention. The α_w and α_s attention mechanisms, which estimate the importance of each hidden

²Note that depending on the number of labels per document the problem can be a multi-label or multi-class problem.

³This statement holds true for multilingual classification problems too if the embeddings are aligned across languages.

state vector, are used to obtain the sentence s_i and document representation h respectively. The sentence vector is thus calculated as follows:

$$s_i = \sum_{t=1}^{T_i} \alpha_w^{(it)} h_w^{(it)} = \sum_{t=1}^{T_i} \frac{\exp(v_{it}^\top u_w)}{\sum_j \exp(v_{ij}^\top u_w)} h_w^{(it)}, \quad (2)$$

where $v_{it} = f_w(h_w^{(it)})$ is a fully-connected network with W_w parameters. The document vector $h \in \mathbb{R}^{d_h}$, where d_h is the dimension of the sentence encoder, is calculated similarly, by replacing u_{it} with $v_i = f_s(h_s^{(i)})$ which is a fully-connected network with W_s parameters, and u_w with u_s , which are parameters of the attention functions.

2.2 Label Text Representation

To encode the label text we use an encoder function which takes as input a label description c_j and outputs a label vector $e_j \in \mathbb{R}^{d_c} \forall j = 1, \dots, k$. For efficiency reasons, we use a simple, parameter-free function to compute e_j , namely the average of word vectors which describe label j , namely $e_j = \frac{1}{L_j} \sum_{t=1}^{L_j} c_{jt}$, and hence $d_c = d$ in this case. By stacking all these label vectors into a matrix, we obtain the label embedding $\mathcal{E} \in \mathbb{R}^{|\mathcal{Y}| \times d}$. In principle, we could also use the same encoder functions as the ones for input text, but this would increase the computation significantly; hence, we keep this direction as future work.

2.3 Output Layer parametrizations

2.3.1 Typical Linear Unit

The most typical output layer, consists of a linear unit with a weight matrix $W \in \mathbb{R}^{d_h \times |\mathcal{Y}|}$ and a bias vector $b \in \mathbb{R}^{|\mathcal{Y}|}$ followed by a softmax or sigmoid activation function. Given the encoder's hidden representation h with dimension size d_h , the probability distribution of output y given input x is proportional to the following quantity:

$$p(y|x) \propto \exp(W^\top h + b). \quad (3)$$

The parameters in W can be learned separately or be tied with the parameters of the embedding E by setting $W = E^T$ if the input dimension of W is restricted to be the same as that of the embedding E ($d = d_h$) and each label is represented by a single word description i.e. when \mathcal{Y} corresponds to \mathcal{V} and $E = \mathcal{E}$. In the latter case, Eq. 3 becomes:

$$p(y|x) \propto \exp(Eh + b). \quad (4)$$

Either way, the parameters of such models are typically learned with cross-entropy loss, which is suitable for classification problems. However, in both cases they cannot be applied to labels which are not seen during training, because each label has learned parameters which are specific to that label, so the parameters for unseen labels cannot be learned. We now turn our focus to a class of models which can handle unseen labels.

2.3.2 Bilinear Input-Label Unit

Joint input-output embedding models can generalize from seen to unseen labels because the parameters of the label encoder are shared. The previously proposed joint input-output embedding models by Yazdani and Henderson (2015) and Nam et al. (2016) are based on the following bilinear ranking function $f(\cdot)$:

$$f(x, y) = \mathcal{E}\mathcal{W}h, \quad (5)$$

where $\mathcal{E} \in \mathbb{R}^{|\mathcal{Y}| \times d}$ is the label embedding and $\mathcal{W} \in \mathbb{R}^{d \times d_h}$ is the bilinear embedding. This function allows one to define the rank of a given label y with respect to x and is trained using hinge loss to rank positive labels higher than negative ones. But note that the use of this ranking loss means that they do not model the conditional probability, as do the traditional models above.

Limitations. Firstly, the above formula can only capture linear relationships between encoded text (h) and label embedding (\mathcal{E}) through \mathcal{W} . We argue that the relationships between different labels are non-linear due to the complex interactions of the semantic relations across labels but also between labels and different encoded inputs. A more appropriate form for this purpose would include a non-linear transformation $\sigma(\cdot)$, e.g. with either:

$$(a) \underbrace{\sigma(\mathcal{E}\mathcal{W})}_{\text{Label structure}} h \quad \text{or} \quad (b) \mathcal{E} \underbrace{\sigma(\mathcal{W}h)}_{\text{Input structure}}. \quad (6)$$

Secondly, it is hard to control their output layer capacity due to their bilinear form, which uses a matrix of parameters (\mathcal{W}) whose size is bounded by the dimensionalities of the label embedding and the text encoding. Thirdly, their loss function optimizes ranking instead of classification performance and thus treats the ground-truth as a ranked list when in reality it consists of one or more independent labels.

Summary. We hypothesize that these are the reasons why these models do not yet perform well on

seen labels compared to models which make use of the typical linear unit, and they do not take full advantage of the structure of the problem when tested on unseen labels. Ideally, we would like to have a model which will address these issues and will combine the benefits from both the typical linear unit and the joint input-label models.

3 The Proposed Output Layer Parametrization for Text Classification

We propose a new output layer parametrization for neural text classification which is comprised of a generalized input-label embedding which captures the structure of the labels, the structure of the encoded texts and the interactions between the two, followed by a classification unit which is independent of the label set size. The resulting model has the following properties: (i) it is able to capture complex output structure, (ii) it has a flexible parametrization which allows its capacity to be controlled, and (iii) it is trained with a classification surrogate loss such as cross-entropy. The model is depicted in Figure 1. In this section, we describe the model in detail, showing how it can be trained efficiently for arbitrarily large label sets and how it is related to previous models.

3.1 A Generalized Input-Label Embedding

Let $g_{in}(h)$ and $g_{out}(e_j)$ be two non-linear projections of the encoded input, i.e. the document h , and any encoded label e_j , where e_j is the j th row vector from the label embedding matrix \mathcal{E} , which have the following form:

$$e'_j = g_{out}(e_j) = \sigma(e_j U + b_u) \quad (7)$$

$$h' = g_{in}(h) = \sigma(Vh + b_v), \quad (8)$$

where $\sigma(\cdot)$ is a nonlinear activation function such as ReLU or Tanh, the matrix $U \in \mathbb{R}^{d \times d_j}$ and bias $b_u \in \mathbb{R}^{d_j}$ are the linear projection of the labels, and the matrix $V \in \mathbb{R}^{d_j \times d_h}$ and bias $b_v \in \mathbb{R}^{d_j}$ are the linear projection of the encoded input. Note that the projections for h' and e'_j could be high-rank or low-rank depending on their initial dimensions and the target joint space dimension. Also let $\mathcal{E}' \in \mathbb{R}^{|\mathcal{Y}| \times d_j}$ be the matrix resulting from projecting all the outputs e_j to the joint space, i.e. $g_{out}(\mathcal{E})$.

The conditional output probability distribution

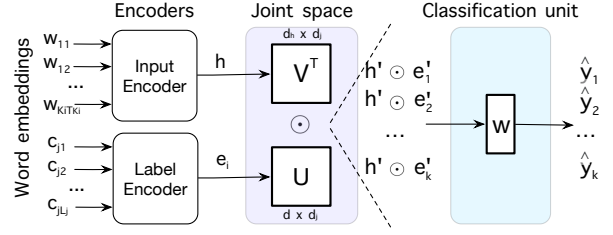


Figure 1: Each encoded text and label are projected to a joint input-label multiplicative space, the output of which is processed by a classification unit with label-set-size independent parametrization.

can now be re-written as:

$$\begin{aligned} p(y|x) &\propto \exp(\mathcal{E}'h') \\ &\propto \exp(g_{out}(\mathcal{E})g_{in}(h)) \\ &\propto \exp(\underbrace{\sigma(\mathcal{E}U + b_u)}_{\text{Label Structure}} \underbrace{\sigma(Vh + b_v)}_{\text{Input Structure}}). \end{aligned} \quad (9)$$

Crucially, this function has no label-set-size dependent parameters, unlike \mathcal{W} and b in Eq. 3. In principle, this parametrization can be used for both multi-class and multi-label problems by defining the exponential in terms of a softmax and sigmoid functions respectively. However, in this paper we will focus on the latter.

3.2 Classification Unit

We require that our classification unit parameters depend only on the joint input-label space above. To represent the compatibility between any encoded input text h_i and any encoded label e_j for this task, we define their joint representation based on multiplicative interactions in the joint space:

$$g_{joint}^{(ij)} = g_{in}(h_i) \odot g_{out}(e_j), \quad (10)$$

where \odot is component-wise multiplication.

The probability for h_i to belong to one of the k known labels is modeled by a linear unit which maps any point in the joint space into a score which indicates the validity of the combination:

$$p_{val}^{(ij)} = g_{joint}^{(ij)} w + b, \quad (11)$$

where $w \in \mathbb{R}^{d_j}$ and b are a scalar variables. We compute the output of this linear unit for each known label which we would like to predict for a given document i , namely:

$$P_{val}^{(i)} = \begin{bmatrix} p_{val}^{(i1)} \\ p_{val}^{(i2)} \\ \dots \\ p_{val}^{(ik)} \end{bmatrix} = \begin{bmatrix} g_{joint}^{(i1)} w + b \\ g_{joint}^{(i2)} w + b \\ \dots \\ g_{joint}^{(ik)} w + b \end{bmatrix}. \quad (12)$$

For each row, the higher the value the more likely the label is to be assigned to the document. To obtain valid probability estimates and be able to train with binary cross-entropy loss for multi-label classification, we apply a sigmoid function as follows:

$$\hat{y}_i = \hat{p}(y_i|x_i) = \frac{1}{1 + e^{-P_{val}^{(i)}}}. \quad (13)$$

Summary. By adding the above changes to the general form of Eq. 9 the conditional probability $p(y_i|x_i)$ is now proportional to the following quantity:

$$\exp(\sigma(\mathcal{E}U + b_u)(\sigma(Vh + b_v) \odot w) + b). \quad (14)$$

Note that the number of parameters in this equation is independent of the size of the label set, given that U , V , w and b depend only on d_j , and k can vary arbitrarily. This allows the model to scale up to large label sets and generalize to unseen labels. Lastly, the proposed output layer addresses all the limitations of the previous models, as follows: (i) it is able to capture complex structure in the joint input-output space, (ii) it provides a means to easily control its capacity d_j , and (iii) it is trainable with cross-entropy loss.

3.3 Training Objectives

The training objective for the multi-label classification task is based on binary cross-entropy loss. Assuming θ contains all the parameters of the model, the training loss is computed as follows:

$$\mathcal{L}(\theta) = -\frac{1}{Nk} \sum_{i=1}^N \sum_{j=1}^k \mathcal{H}(y_{ij}, \hat{y}_{ij}), \quad (15)$$

where \mathcal{H} is the binary cross-entropy between the gold label y_{ij} and predicted label \hat{y}_{ij} for a document i and a candidate label j .

We handle multiple languages according to [Firat et al. \(2016\)](#) and [Pappas and Popescu-Belis \(2017\)](#). Assuming that $\Theta = \{\theta_1, \theta_2, \dots, \theta_M\}$ are all the parameters required for each of the M languages, we use a joint multilingual objective based on the sum of cross-entropy losses:

$$\mathcal{L}(\Theta) = -\frac{1}{Z} \sum_i^{N_e} \sum_l^M \sum_{j=1}^k \mathcal{H}(y_{ij}^{(l)}, \hat{y}_{ij}^{(l)}), \quad (16)$$

where $Z = N_e M k$ with N_e being the number of examples per epoch. At each iteration,

a document-label pair for each language is sampled. In addition, multilingual models share a certain subset of the encoder parameters during training while the output layer parameters are kept language-specific, as described by [Pappas and Popescu-Belis \(2017\)](#). In this paper, we share most of the output layer parameters, namely the ones from the input-label space (U , V , b_v , b_u), and we keep only the classification unit parameters (w , b) language-specific.

3.4 Scaling Up to Large Label Sets

For a very large number d_j of joint-space dimensions in our parametrization, the computational complexity increases prohibitively because our projection requires a large matrix multiplication between U and E , which depends on $|\mathcal{Y}|$. In such cases, we resort to sampling-based training, by adopting the commonly used negative sampling method proposed by [Mikolov et al. \(2013\)](#). Let $x_i \in \mathbb{R}^d$ and $y_{ik} \in \{0, 1\}$ be an input-label pair and \hat{y}_{ik} the output probabilities from our model (Eq. 14). By introducing the sets k_i^p and k_i^n , which contain the indices of the positive and negative labels respectively for the i -th input, the loss $L(\theta)$ in Eq. 15 can be re-written as follows:

$$\begin{aligned} &= -\frac{1}{Z} \sum_{i=1}^N \sum_{j=1}^k \left[y_{ij} \log \hat{y}_{ij} + \bar{y}_{ij} \log (1 - \hat{y}_{ij}) \right] \\ &= -\frac{1}{Z} \sum_{i=1}^N \left[\sum_{j=1}^{k_i^p} \log \hat{y}_{ij} + \sum_{j=1}^{k_i^n} \log (1 - \hat{y}_{ij}) \right], \end{aligned} \quad (17)$$

where $Z = Nk$ and \bar{y}_{ij} is $(1 - y_{ij})$. To reduce the computational cost needed to evaluate \hat{y}_{ij} for all the negative label set k_i^n , we sample k^* labels from the negative label set with probability $p = \frac{1}{|k_i^n|}$ to create the set k_i^{n*} . This enables training on arbitrarily big label sets without increasing the computation required. By controlling the number of samples we can drastically speed up the training time, as we demonstrate empirically in Section 4.2.2. Exploring more informative sampling methods, e.g. importance sampling, would be an interesting direction of future work.

3.5 Relation to Previous Parametrizations

The proposed embedding form can be seen as a generalization over the input-label embeddings with a bilinear form, because its degenerate form

is equivalent to the bilinear form of Eq. 5. In particular, this can be simply derived if we set one of the two non-linear projection functions in the second line of Eq. 9 to be the identity function, e.g. $g_{out}(\cdot) = I$, set all biases to zero, and make the $\sigma(\cdot)$ activation function linear, as follows:

$$\begin{aligned} \sigma(\mathcal{E}U + b_u)\sigma(Vh + b_v) &= (\mathcal{E}I)(Vh) \\ &= \mathcal{E}Vh \quad \square, \end{aligned} \quad (18)$$

where V by consequence has the same number of dimensions as $\mathcal{W} \in \mathbb{R}^{d \times d_h}$ from the bilinear input-label embedding model of Eq. 5.

4 Experiments

The evaluation is performed on large-scale biomedical semantic indexing using the BioASQ dataset, obtained by Nam et al. (2016), and on multilingual news classification using the DW corpus, which consists of eight language datasets obtained by Pappas and Popescu-Belis (2017). The statistics of these datasets are listed in Table 1.

4.1 Biomedical Text Classification

We evaluate on biomedical text classification to demonstrate that our generalized input-label model scales to very large label sets and performs better than previous joint input-label models on both seen and unseen label prediction scenarios.

4.1.1 Settings

We follow the exact evaluation protocol, data and settings of Nam et al. (2016), as described below. We use the BioASQ Task 3a dataset, which is a collection of scientific publications in biomedical research. The dataset contains about 12M documents labeled with around 11 labels out of 27,455, which are defined according to the Medical Subject Headings (MESH) hierarchy. The data was minimally pre-processed with tokenization, number replacements (NUM), rare word replacements (UNK), and split with the provided script by year so that the training set includes all documents until 2004 and the ones from 2005 to 2015 were kept for the test set, this corresponded to 6,692,815 documents for training and 4,912,719 for testing. For validation, a set of 100,000 documents were randomly sampled from the training set. We report the same ranking-based evaluation metrics as Nam et al. (2016), namely rank loss (RL), average precision (AvgPr) and one-error loss (OneErr).

Dataset abbrev.	Documents			Labels	
	# count	# words	\bar{w}_d	# count	\bar{w}_l
BioASQ	11,705,534	528,156	214	26,104	35.0
DW	598,304	884,272	436	5,637	2.3
- en	112,816	110,971	516	1,385	2.1
- de	132,709	261,280	424	1,176	1.8
- es	75,827	130,661	412	843	4.7
- pt	39,474	58,849	571	396	1.8
- uk	35,423	105,240	342	288	1.7
- ru	108,076	123,493	330	916	1.8
- ar	57,697	58,922	357	435	2.4
- fa	36,282	34,856	538	198	2.5

Table 1: Dataset statistics: #count is the number of documents, #words are the number of unique words in the vocabulary \mathcal{V} , \bar{w}_d and \bar{w}_l are the average number of words per document and label respectively.

Our hyper-parameters were selected on validation data based on average precision as follows: 100-dimensional word embeddings, encoder, attention (same dimensions as the baselines), joint input-label embedding of 500, batch size of 64, maximum number of 300 words per document and 50 words per label, ReLU activation, 0.3% negative label sampling, and optimization with ADAM until convergence. The word embeddings were learned end-to-end on the task.⁴

The baselines are the joint input-label models from Nam et al. (2016), noted as [N16], namely:

- **WSABIE+**: This model is an extension of the original WSABIE model by Weston et al. (2011), which instead of learning a ranking model with fixed document features, it jointly learns features for documents and words, and is trained with the WARP ranking loss.
- **AiTextML**: This model is the one proposed by Nam et al. (2016) with the purpose of learning jointly representations of documents, labels and words, along with a joint input-label space which is trained with the WARP ranking loss.

The scores of the WSABIE+ and AiTextML baselines in Table 2 are the ones reported by Nam et al. (2016). In addition, we report scores of a word-level attention neural network (WAN) with DENSE encoder and attention followed by a sigmoid out-

⁴Here, the word embeddings are included in the parameter statistics because they are variables of the network.

	Model abbrev.	Layer form output	Dim #count	Seen labels			Unseen labels			Params #count
				RL	AvgPr	OneErr	RL	AvgPr	OneErr	
[N16]	WSABIE+	$\mathcal{E}Wh_t$	100	5.21	36.64	41.72	48.81	0.37	99.94	722.10M
	AiTextML avg	$\mathcal{E}Wh_t$	100	3.54	32.78	25.99	52.89	0.39	99.94	724.47M
	AiTextML inf	$\mathcal{E}Wh_t$	100	3.54	32.78	25.99	21.62	2.66	98.61	724.47M
Baselines	WAN	$W^\top h_t$	–	1.53	42.37	11.23	–	–	–	55.60M
	BIL-WAN [YH15]	$\sigma(\mathcal{E}W)Wh_t$	100	1.21	40.68	17.52	18.72	9.50	93.89	52.85M
	BIL-WAN [N16]	$\mathcal{E}Wh_t$	100	1.12	41.91	16.94	16.26	10.55	93.23	52.84M
	GILE-WAN	$\sigma(\mathcal{E}U)\sigma(Vh_t)$	500	0.78	44.39	11.60	9.06	12.95	91.90	52.93M
Ours	– constrained d_j	$\sigma(\mathcal{E}W)\sigma(\mathcal{W}h_t)$	100	1.01	37.71	16.16	10.34	11.21	93.38	52.85M
	– only label (Eq. 6a)	$\sigma(\mathcal{E}W)h_t$	100	1.06	40.81	13.77	9.77	14.71	90.56	52.84M
	– only input (Eq. 6b)	$\mathcal{E}\sigma(\mathcal{W}h_t)$	100	1.07	39.78	15.67	19.28	7.18	95.91	52.84M

Table 2: Biomedical semantic indexing results computed over labels seen and unseen during training, i.e. the full-resource versus zero-resource settings. Best scores among the competing models are marked in **bold**.

put layer, trained with binary cross-entropy loss.⁵ Our model replaces WAN’s output layer with a generalized input-label embedding layer and its variations, noted GILE-WAN. For comparison, we also compare to bilinear input-label embedding versions of WAN for the model by Yazdani and Henderson (2015), noted as BIL-WAN [YH16], and the one by Nam et al. (2016), noted as BIL-WAN [N16]. Note that the AiTextML parameter space is huge and makes learning difficult for our models (linear wrt. labels and documents). Instead, we make sure that our models have far fewer parameters than the baselines (Table 2).

4.1.2 Results

The results on biomedical semantic indexing on seen and unseen labels are shown in Table 2. We observe that the neural baseline, WAN, outperforms WSABIE+ and AiTextML on the seen labels, namely by +5.73 and +9.59 points in terms of AvgPr respectively. The differences are even more pronounced when considering the ranking loss and one error metrics. This result is compatible with previous findings that existing joint input-label models are not able to outperform strong supervised baselines on seen labels. However, WAN is not able to generalize at all to unseen labels, hence the WSABIE+ and AiTextML have a clear advantage in the zero-resource setting.

In contrast, our generalized input-label model,

⁵ In our preliminary experiments, we also trained the neural model with a hinge loss as WSABIE+ and AiTextML, but it performed similarly to them and much worse than WAN, so we did not further experiment with it.

GILE-WAN, outperforms WAN even on seen labels, where our model has higher average precision by +2.02 points, better ranking loss by +43% and comparable OneErr (−3%). And this gain is not at the expense of performance on unseen labels. GILE-WAN, outperforms WSABIE+, AiTextML variants⁶ by a large margin in both cases, e.g. by +7.75, +11.61 points on seen labels and by +12.58, +10.29 points in terms of average precision on unseen labels, respectively. Interestingly, our GILE-WAN model also outperforms the two previous bilinear input-label embedding formulations of Yazdani and Henderson (2015) and Nam et al. (2016), namely BIL-WAN [YH15] and BIL-WAN [N16] by +3.71, +2.48 points on seen labels and +3.45 and +2.39 points on unseen labels, respectively, even when they are trained with the same encoders and loss as ours. These models are not able to outperform the WAN baseline when evaluated on the seen labels, namely they have −1.68 and −0.46 points lower average precision than WAN, but they outperform WSABIE+ and AiTextML on both seen and unseen labels. Overall, the results show a clear advantage of our generalized input-label embedding model against previous models on both seen and unseen labels.

4.1.3 Ablation Analysis

To evaluate the effectiveness of individual components of our model, we performed an ablation study (last three rows in Table 2). Note that when we use only the label or only the input embedding

⁶Namely, *avg* when using the average of word vectors and *inf* when using inferred label vectors to make predictions.

in our generalized input-label formulation, the dimensionality of the joint space is constrained to be the dimensionality of the encoded labels and inputs respectively, that is $d_j=100$ in our experiments.

All three variants of our model outperform previous embedding formulations of Nam et al. (2016) and Yazdani and Henderson (2015) in all metrics except from AvgPr on seen labels where they score slightly lower. The decrease in AvgPrec for our model variants with $d_j=100$ compared to the neural baselines could be attributed to the difficulty in learning the parameters of a highly non-linear space with only a few hidden dimensions. Indeed, when we increase the number of dimensions ($d_j=500$), our full model outperforms them by a large margin. Recall that this increase in capacity is only possible with our full model definition in Eq. 9 and none of the other variants allow us to do this without interfering with the original dimensionality of the encoded labels (\mathcal{E}) and input (h_t). In addition, our model variants with $d_j=100$ exhibit consistently higher scores than baselines in terms of most metrics on both seen and unseen labels, which suggests that they are able to capture more complex relationships across labels and between encoded inputs and labels.

Overall, the best performance among our model variants is achieved when using only the label embedding and, hence, it is the most significant component of our model. Surprisingly, our model with only the label embedding achieves higher performance than our full model on unseen labels but it is far behind our full model when we consider performance on both seen and unseen labels. When we constrain our full model to have the same dimensionality with the other variants, i.e. $d_j=100$, it outperforms the one that uses only the input embedding in most metrics and it is outperformed by the one that uses only the label embedding.

4.2 Multilingual News Text Classification

We evaluate on multilingual news text classification to demonstrate that our output layer based on the generalized input-label embedding outperforms previous models with a typical output layer in a wide variety of settings, even for labels which have been seen during training.

4.2.1 Settings

We follow the exact evaluation protocol, data and settings of Pappas and Popescu-Belis (2017), as

described below. The dataset is split per language into 80% for training, 10% for validation and 10% for testing. We evaluate on both types of labels (general Y_g , and specific Y_s) in a *full-resource scenario*, and we evaluate only on the general labels (Y_g) in a *low-resource scenario*. Accuracy is measured with the micro-averaged F1 percentage scores.

The word embeddings for this task are the aligned pre-trained 40-dimensional multi-CCA multilingual word embeddings by Ammar et al. (2016) and are kept fixed during training.⁷ The sentences are already truncated at a length of 30 words and the documents at a length of 30 sentences. The hyper-parameters were selected on validation data as follows: 100-dimensional encoder and attention, ReLU activation, batch size of 16, epoch size of 25k, no negative sampling (all labels are used) and optimization with ADAM until convergence. To ensure equal capacity to baselines, we use approximately the same number of parameters n_{tot} with the baseline classification layers, by setting:

$$d_j \simeq \frac{d_h * |k^{(i)}|}{d_h + d}, \quad i = 1, \dots, M, \quad (19)$$

in the monolingual case, and similarly, $d_j \simeq (d_h * \sum_{i=1}^M |k^{(i)}|) / (d_h + d)$ in the multilingual case, where $k^{(i)}$ is the number of labels in language i .

The hierarchical models have *Dense* encoders in all scenarios (Tables 3, 6, and 7), except from the varying encoder experiment (Table 4). For the low-resource scenario, the levels of data availability are: *tiny* from 0.1% to 0.5%, *small* from 1% to 5% and *medium* from 10% to 50% of the original training set. For each level, the average F1 across discrete increments of 0.1, 1 and 10 are reported respectively. The decision thresholds, which were tuned on validation data by Pappas and Popescu-Belis (2017), are set as follows: for the full-resource scenario it is set to 0.4 for $|Y_s| < 400$ and 0.2 for $|Y_s| \geq 400$, and for the low-resource scenario it is set to 0.3 for all sets.

The baselines are all the monolingual and multilingual neural networks from Pappas and Popescu-Belis (2017)⁸, noted as [PB17], namely:

⁷The word embeddings are not included in the parameters statistics because they are not variables of the network.

⁸For reference, in Table 4 we also compare to a logistic regression trained with unigrams over the full vocabulary and

Y_g	Models abbrev.	Languages (en + aux → en)							Languages (en + aux → aux)							Stat. <i>avg</i>
		de	es	pt	uk	ru	ar	fa	de	es	pt	uk	ru	ar	fa	
[PB17]	Mono NN (Avg)	50.7	53.1	70.0	57.2	80.9	59.3	64.4	66.6	57.6
	Mono HNN (Avg)	70.0	67.9	82.5	70.5	86.8	77.4	79.0	76.6	73.6
	Mono HAN (Att)	71.2	71.8	82.8	71.3	85.3	79.8	80.5	76.6	74.7
	Multi MHAN-Enc	71.0	69.9	69.2	70.8	71.5	70.0	71.3	69.7	82.9	69.7	86.8	80.3	79.0	76.0	74.1
	Multi MHAN-Att	74.0	74.2	74.1	72.9	73.9	73.8	73.3	72.5	82.5	70.8	87.7	80.5	82.1	76.3	<u>76.3</u>
	Multi MHAN-Both	72.8	71.2	70.5	65.6	71.1	68.9	69.2	70.4	82.8	71.6	87.5	80.8	79.1	77.1	74.2
Ours	Mono GILE-NN (Avg)	60.1	60.3	76.6	62.1	82.0	65.7	77.4	68.6	65.2
	Mono GILE-HNN (Avg)	74.8	71.3	83.3	72.6	88.3	81.5	81.9	77.1	77.1
	Mono GILE-HAN (Att)	76.5	74.2	83.4	71.9	86.1	82.7	81.0	77.2	78.0
	Multi GILE-MHAN-Enc	75.1	74.0	72.7	70.7	74.4	73.5	73.2	72.7	83.4	73.0	88.7	82.8	83.3	77.4	76.7
	Multi GILE-MHAN-Att	76.5	76.5	76.3	75.3	76.1	75.6	75.2	74.5	83.5	72.7	88.0	83.4	82.1	76.7	78.0
	Multi GILE-MHAN-Both	75.3	73.7	72.1	67.2	72.5	73.8	69.7	72.6	84.0	73.5	89.0	81.9	82.0	77.7	76.0
Y_s	Models	de	es	pt	uk	ru	ar	fa	de	es	pt	uk	ru	ar	fa	<i>avg</i>
[PB17]	Mono NN (Avg)	24.4	21.8	22.1	24.3	33.0	26.0	24.1	32.1	25.3
	Mono HNN (Avg)	39.3	39.6	37.9	33.6	42.2	39.3	34.6	43.1	38.9
	Mono HAN (Att)	43.4	44.8	46.3	41.9	46.4	45.8	41.2	49.4	44.2
	Multi MHAN-Enc	45.4	45.9	44.3	41.1	42.1	44.9	41.0	43.9	46.2	39.3	47.4	45.0	37.9	48.6	43.8
	Multi MHAN-Att	46.3	46.0	45.9	45.6	46.4	46.4	46.1	46.5	46.7	43.3	47.9	45.8	41.3	48.0	<u>45.8</u>
	Multi MHAN-Both	45.7	45.6	41.5	41.2	45.6	44.6	43.0	45.9	46.4	40.3	46.3	46.1	40.7	50.3	44.5
Ours	Mono GILE-NN (Avg)	27.5	27.5	28.4	29.2	36.8	31.6	32.1	35.6	29.5
	Mono GILE-HNN (Avg)	43.1	43.4	42.0	37.7	43.0	42.9	36.6	44.1	42.2
	Mono GILE-HAN (Att)	45.9	47.3	47.4	42.6	46.6	46.9	41.9	48.6	45.9
	Multi GILE-MHAN-Enc	46.0	46.6	41.2	42.5	46.4	43.4	41.8	47.2	47.7	41.5	49.5	46.6	41.4	50.7	45.1
	Multi GILE-MHAN-Att	47.3	47.0	45.8	45.5	46.2	46.5	45.5	47.6	47.9	43.5	49.1	46.5	42.2	50.3	<u>46.5</u>
	Multi GILE-MHAN-Both	47.0	46.7	42.8	42.0	45.6	42.8	39.3	48.0	47.6	43.1	48.5	46.0	42.1	49.0	45.0

Table 3: Full-resource classification results on general (upper half) and specific (lower half) labels using monolingual and bilingual models with DENSE encoders on English as target (left) and the auxiliary language as target (right). The average bilingual F1-score (%) is noted *avg* and the top ones per block are underlined. The monolingual scores on the left come from a single model, hence a single score is repeated multiple times; the repetition is marked with consecutive dots.

- **NN**: A neural network which feeds the average vector of the input words directly to a classification layer, as the one used by [Klementiev et al. \(2012\)](#).
- **HNN**: A hierarchical network with encoders and average pooling at every level, followed by a classification layer, as the one used by [Tang et al. \(2015\)](#).
- **HAN**: A hierarchical network with encoders and attention, followed by a classification layer, as the one used by [Yang et al. \(2016\)](#).
- **MHAN**: Three multilingual hierarchical networks with shared encoders, noted MHAN-Enc, shared attention, noted MHAN-Att, and shared attention and encoders, noted MHAN-Both, as the ones used by [Pappas and Popescu-Belis \(2017\)](#).

To ensure a controlled comparison to the above baselines, for each model we evaluate a version where their output layer is replaced by our generalized input-label embedding output layer over the top-10% most frequent words by [Mrini et al. \(2017\)](#), noted as [M17], which use the same settings and data.

using the same number of parameters; these have the abbreviation “GILE” prepended in their name (e.g. GILE-HAN). The scores of HAN and MHAN models in Tables 3, 6 and 7 are the ones reported by [Pappas and Popescu-Belis \(2017\)](#), while for Table 4 we train them ourselves using their code. Lastly, the best score for each pairwise comparison between a joint input-label model and its counterpart is marked in **bold**.

4.2.2 Results

Table 3 displays the results of full-resource document classification using DENSE encoders for both general and specific labels. On the left, we display the performance of models on the English sub-corpus when English and an auxiliary language are used for training, and on the right, the performance on the auxiliary language sub-corpus when that language and English are used for training.

The results show that in 98% of comparisons on general labels (top half of Table 3) the joint input-label models improve consistently over the corresponding models using a typical sigmoid classification layer. This finding validates our main hypothesis that the joint input-label models suc-

Models		Languages								Statistics	
abbrev.		en	de	es	pt	uk	ru	ar	fa	n_l	f_l
[M17]	LogReg-BOW	75.8	72.9	81.4	74.3	91.0	79.2	82.0	77.0	26M	79.19
	LogReg-BOW-10%	74.7	70.1	80.6	71.1	89.5	76.5	80.8	75.5	5M	77.35
[PB17]	HAN-BIGRU	76.3	74.1	84.5	72.9	87.7	82.9	81.7	75.3	377K	79.42
	HAN-GRU	77.1	72.5	84.0	70.8	86.6	83.0	82.9	76.0	138K	79.11
	HAN-DENSE	71.2	71.8	82.8	71.3	85.3	79.8	80.5	76.6	50K	77.41
Ours	GILE-HAN-BIGRU	78.1	73.6	84.9	72.5	89.0	82.4	82.5	75.8	377K	79.85
	GILE-HAN-GRU	77.1	72.6	84.7	72.4	88.6	83.6	83.4	76.0	138K	79.80
	GILE-HAN-DENSE	76.5	74.2	83.4	71.9	86.1	82.7	82.6	77.2	50K	79.12

Table 4: Full-resource classification results on general (Y_g) topic labels with DENSE and GRU encoders. Reported are also the average number of parameters per language (n_l), and the average F_1 per language (f_l).

cessfully exploit the semantics of the labels, which provide useful cues for classification, as opposed to models which are agnostic to label semantics. The results for specific labels (bottom half of Table 3) demonstrate the same trend, with the joint input-label models performing better in 87% of comparisons.

In Table 5, we also directly compare our embedding to previous bilinear input-label embedding formulations when using the best monolingual configuration (HAN) from Table 3, exactly as done in Section 4.1. The results on the general labels show that GILE outperforms the previous bilinear input-label models, BIL [YH15] and BIL [N16], by +1.62 and +3.3 percentage points on average respectively. This difference is much more pronounced on the specific labels, where the label set is much larger, namely +6.5 and +13.5 percentage points respectively. Similarly, our model with constrained dimensionality is also as good or better on average than the bilinear input-label models, by +0.9 and +2.2 on general labels and by -0.5 and +6.1 on specific labels respectively, which highlights the importance of learning non-linear relationships across encoded labels and documents. Among our ablated model variants, as in previous section, the best is the one with only the label projection but it still worse than our full model by -5.2 percentage points. The improvements of GILE against each baseline is significant and consistent on both datasets. Hence, in the following experiments we will only consider the best of these alternatives.

The best bilingual performance on average is that of the GILE-MHAN-Att model, for both general and specific labels. This improvement can be attributed to the effective sharing between la-

HAN	Languages							
Y_g output layer	en	de	es	pt	uk	ru	ar	fa
Linear [PB17]	71.2	71.8	82.8	71.3	85.3	79.8	80.5	76.6
BIL [YH15]	71.7	70.5	82.0	71.1	86.6	80.6	80.4	76.0
BIL [N16]	69.8	69.1	80.9	67.4	87.5	79.9	78.4	75.1
GILE (Ours)	76.5	74.2	83.4	71.9	86.1	82.7	82.6	77.2
- constrained d_j	73.6	73.1	83.3	71.0	87.1	81.6	80.4	76.4
- only label	71.4	69.6	82.1	70.3	86.2	80.6	81.1	76.2
- only input	55.1	54.2	80.6	66.5	85.6	60.8	78.9	74.0
Y_s output layer	en	de	es	pt	uk	ru	ar	fa
Linear [PB17]	43.4	44.8	46.3	41.9	46.4	45.8	41.2	49.4
BIL [YH15]	40.7	37.8	38.1	33.5	44.6	38.1	39.1	42.6
BIL [N16]	34.4	30.2	34.4	33.6	31.4	22.8	35.6	38.9
GILE (Ours)	45.9	47.3	47.4	42.6	46.6	46.9	41.9	48.6
- constrained d_j	38.5	38.0	36.8	35.1	42.1	36.1	36.7	48.7
- only label	38.4	41.5	42.9	38.3	44.0	39.3	37.2	43.4
- only input	12.1	10.8	8.8	20.5	11.8	7.8	12.0	24.6

Table 5: Direct comparison with previous bilinear input-label models, namely BIL [YH15] and BIL [N16], and with our ablated model variants using the best monolingual configuration (HAN) from Table 3 on both general (upper half) and specific (lower half) labels. Best scores among the competing models are marked in **bold**.

bel semantics across languages through the joint multilingual input-label output layer. Effectively, this model has the same multilingual sharing scheme with the best model reported by Pappas and Popescu-Belis (2017), MHAN-Att, namely sharing attention at each level of the hierarchy, which agrees well with their main finding. Interestingly, the improvement holds when using different types of hierarchical encoders, namely

Models		General labels		Specific labels	
abbrev.	# lang.	n_l	f_l	n_l	f_l
[PB17]	HAN	1	50K 77.41	90K 44.90	
	MHAN	2	40K 78.30	80K 45.72	
	MHAN	8	32K 77.91	72K 45.82	
Ours	GILE-HAN	1	50K 79.12	90K 45.90	
	GILE-MHAN	2	40K 79.68	80K 46.49	
	GILE-MHAN	8	32K 79.48	72K 46.32	

Table 6: Multilingual learning results. The columns are the average number of parameters per language (n_l), average F_1 per language (f_l).

DENSE GRU, and biGRU, as shown in Table 4, which demonstrate the generality of the approach. In addition, our best models outperform logistic regression trained either on top-10% most frequent words or on the full vocabulary, even though our models utilize many fewer parameters, namely 377K/138K vs. 26M/5M. Increasing the capacity of our models should lead to even further improvements.

Multilingual learning. So far, we have shown that the proposed joint input-label models outperform typical neural models when training with one and two languages. Does the improvement remain when increasing the number of languages even more? To answer the question we report in Table 6 the average F1-score per language for the best baselines from the previous experiment (HAN and MHAN-Att) with the proposed joint input-label versions of them (GILE-HAN and GILE-MHAN-Att) when increasing the number of languages (1, 2 and 8) that are used for training. Overall, we observe that the joint input-label models outperform all the baselines independently of the number of languages involved in the training, while having the same number of parameters. We also replicate the previous result that a second language helps but beyond that there is no improvement.

Low-resource transfer. We investigate here whether joint input-label models are useful for low-resource languages. Table 7 shows the low-resource classification results from English to seven other languages when varying the amount of their training data. Our model with both shared encoders and attention, GILE-MHAN, outperforms previous models in average, namely HAN (Yang et al., 2016) and MHAN (Pappas and Popescu-Belis, 2017), for low-resource classification in the majority of the cases.

	Levels range	[PB17]		Ours
		HAN	MHAN	GILE-MHAN
en → de	0.1-0.5%	29.9	39.4	42.9
	1-5%	51.3	52.6	51.6
	10-50%	63.5	63.8	65.9
en → es	0.1-0.5%	39.5	41.5	39.0
	1-5%	45.6	50.1	50.9
	10-50%	74.2	75.2	76.4
en → pt	0.1-0.5%	30.9	33.8	39.6
	1-5%	44.6	47.3	48.9
	10-50%	60.9	62.1	62.3
en → uk	0.1-0.5%	60.4	60.9	61.1
	1-5%	68.2	69.0	69.4
	10-50%	76.4	76.7	76.5
en → ru	0.1-0.5%	27.6	29.1	27.9
	1-5%	39.3	40.2	40.2
	10-50%	69.2	69.4	70.4
en → ar	0.1-0.5%	35.4	36.6	46.1
	1-5%	45.6	46.6	49.5
	10-50%	48.9	47.8	61.8
en → fa	0.1-0.5%	36.0	41.3	42.5
	1-5%	55.0	55.5	55.4
	10-50%	69.2	70.0	69.7

Table 7: Low-resource classification results with various sizes of training data using the general labels.

The shared input-label space appears to be helpful especially when transferring from English to German, Portuguese and Arabic languages. GILE-MHAN is significantly behind MHAN on transferring knowledge from English to Spanish and to Russian in the 0.1-0.5% resource setting, but in the rest of the cases they have very similar scores.

Label sampling. To speedup computation it is possible to train our model by sampling labels, instead of training over the whole label set. How much speed-up can we achieve from this label sampling approach and still retain good levels of performance? In Figure 2, we attempt to answer this question by reporting the performance of our GILE-HNN model when varying the amount of labels (%) that it uses for training over English general and specific labels of the DW dataset. In both cases, the performance of GILE-HNN tends to increase as the percentage of labels sampled increases, but it levels off for the higher percentages.

For general labels, top performance is reached with a 40% to 50% sampling rate, which translates to a 22% to 18% speedup, while for the specific labels, it is reached with a 60% to 70% sampling rate, which translates to a 40% to 36% speedup.

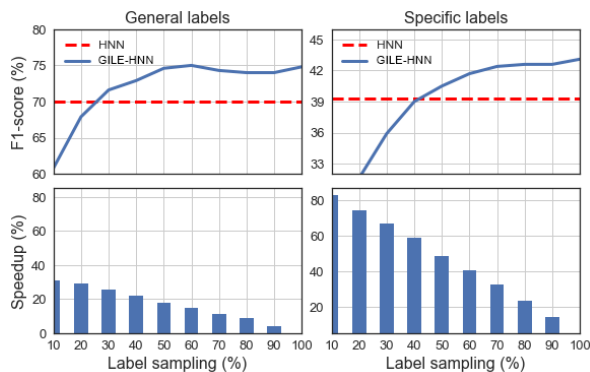


Figure 2: Varying sampling percentage for general and specific English labels. (*Top*) GILE-HNN is compared against HNN in terms of F1 (%). (*Bottom*) The runtime speedup over GILE-HNN trained on the full label set.

The speedup is correlated to the size of the label set, since there are many fewer general labels than specific labels, namely 327 vs 1,058 here. Hence, we expect even higher speedups for bigger label sets. Interestingly, GILE-HNN with label sampling reaches the performance of the baseline with a 25% and 60% sample for general and specific labels respectively. This translates to a speedup of 30% and 50% respectively compared to a GILE-HNN trained over all labels. Overall, these results show that our model is effective and that it can also scale to large label sets. The label sampling should also be useful in tasks where the computation resources may be limited or budgeted.

5 Related Work

5.1 Neural text Classification

Research in *neural text classification* was initially based on feed-forward networks, which required unsupervised pre-training (Collobert et al., 2011; Mikolov et al., 2013; Le and Mikolov, 2014) and later on they focused on networks with hierarchical structure. Kim (2014) proposed a convolutional neural network (CNN) for sentence classification. Johnson and Zhang (2015) proposed a CNN for high-dimensional data classification, while Zhang et al. (2015) adopted a character-level CNN for text classification. Lai et al. (2015) proposed a recurrent CNN to capture sequential information, which outperformed simpler CNNs. Lin et al. (2015) and Tang et al. (2015) proposed hierarchical recurrent neural networks and showed that they were superior to CNN-based models. Yang et al. (2016) demonstrated that a hierarchical attention network with bi-directional gated en-

coders outperforms previous alternatives. Pappas and Popescu-Belis (2017) adapted such networks to learn hierarchical document structures with shared components across different languages.

The issue of scaling to large label sets has been addressed previously by output layer approximations (Morin and Bengio, 2005) and with the use of sub-word units or character-level modeling (Sennrich et al., 2016; Lee et al., 2017) which is mainly applicable to structured prediction problems. Despite the numerous studies, most of the existing neural text classification models ignore label descriptions and semantics. Moreover, they are based on typical output layer parametrizations which are dependent on the label set size, and thus are not able to scale well to large label sets nor to generalize to unseen labels. Our output layer parametrization addresses these limitations and could potentially improve such models.

5.2 Output Representation Learning

There exist studies which aim to learn output representations directly from data without any semantic grounding to word embeddings (Srikumar and Manning, 2014; Yeh et al., 2018; Augenstein et al., 2018). Such methods have a label-set-size dependent parametrization, which makes them data hungry, less scalable on large label sets and incapable of generalizing to unseen classes. Wang et al. (2018) addressed the lack of semantic grounding to word embeddings by proposing an efficient method based on label-attentive text representations which are helpful for text classification. However, in contrast to our study, their parametrization is still label-set-size dependent and thus their model is not able to scale well to large label sets nor to generalize to unseen labels.

5.3 Zero-shot Text Classification

Several studies have focused on learning joint input-label representations grounded to word semantics for unseen label prediction for images (Weston et al., 2011; Socher et al., 2013; Norouzi et al., 2014; Zhang et al., 2016; Fu et al., 2018), called zero-shot classification. However, there are fewer such studies for text classification. Dauphin et al. (2014) predicted semantic utterances of text by mapping them in the same semantic space with the class labels using an unsupervised learning objective. Yazdani and Henderson (2015) proposed a zero-shot spoken language understanding model based on a bilinear input-label model able to gen-

eralize to previously unseen labels. Nam et al. (2016), proposed a bilinear joint document-label embedding which learns shared word representations between documents and labels. More recently, Shu et al. (2017) proposed an approach for open-world classification which aims to identify novel documents during testing but it is not able to generalize to unseen classes. Perhaps, the most similar model to ours is from the recent study by Pappas et al. (2018) on neural machine translation, with the difference that they have single-word label descriptions and they use a label-set-dependent bias in a softmax linear prediction unit, which is designed for structured prediction. Hence, their model can neither handle unseen labels nor multi-label classification, as we do here.

Compared to previous joint input-label models, the proposed model has a more general and flexible parametrization which allows the output layer capacity to be controlled. Moreover, it is not restricted to linear mappings, which have limited expressivity, but uses nonlinear mappings, similar to energy-based learning networks (LeCun et al., 2006; Belanger and McCallum, 2016). The link to the latter can be made if we regard $P_{val}^{(ij)}$ in Eq. 11 as an energy function for the i -th document and the j -th label, the calculation of which uses a simple multiplicative transformation (Eq. 10). Lastly, the proposed model performs well on both seen and unseen label sets by leveraging the binary cross-entropy loss, which is the standard loss for classification problems, instead of a ranking loss.

6 Conclusion

We proposed a novel joint input-label embedding model for neural text classification which generalizes over existing input-label models and addresses their limitations while preserving high performance on both seen and unseen labels. Compared to baseline neural models with a typical output layer, our model is more scalable and has better performance on the seen labels. Compared to previous joint input-label models, it performs significantly better on unseen labels without compromising performance on the seen labels. These improvements can be attributed to the the ability of our model to capture complex input-label relationships, to its controllable capacity and to its training objective which is based on cross-entropy loss.

As future work, the label representation could be learned by a more sophisticated encoder, and

the label sampling could benefit from importance sampling to avoid revisiting uninformative labels. Another interesting direction would be to find a more scalable way of increasing the output layer capacity, for instance using a deep rather than wide classification network. Moreover, adapting the proposed model to structured prediction, for instance by using a softmax classification unit instead of a sigmoid one, would benefit tasks such as neural machine translation, language modeling and summarization, in isolation but also when trained jointly with multi-task learning.

Acknowledgments

We are grateful for the support from the European Union through its Horizon 2020 program in the SUMMA project n. 688139, see <http://www.summa-project.eu>. We would also like to thank our action editor, Eneko Agirre, and the anonymous reviewers for their invaluable suggestions and feedback.

References

- Waleed Ammar, George Mulcaire, Yulia Tsvetkov, Guillaume Lample, Chris Dyer, and Noah A. Smith. 2016. [Massively multilingual word embeddings](#). *CoRR*, abs/1602.01925.v2.
- Isabelle Augenstein, Sebastian Ruder, and Anders Søgaard. 2018. [Multi-task learning of pairwise sequence classification tasks over disparate label spaces](#). In *Proceedings of the 2018 Conference of the North American Chapter of the Association for Computational Linguistics: Human Language Technologies, Volume 1 (Long Papers)*, pages 1896–1906, New Orleans, Louisiana.
- David Belanger and Andrew McCallum. 2016. [Structured prediction energy networks](#). In *Proceedings of The 33rd International Conference on Machine Learning*, volume 48 of *Proceedings of Machine Learning Research*, pages 983–992, New York, New York, USA. PMLR.
- Jianshu Chen, Ji He, Yelong Shen, Lin Xiao, Xiaodong He, Jianfeng Gao, Xinying Song, and Li Deng. 2015. [End-to-end learning of LDA by mirror-descent back propagation over a deep architecture](#). In *Advances in Neural Information Processing Systems 28*, pages 1765–1773, Montreal, Canada.

- Kyunghyun Cho, Bart van Merriënboer, Caglar Gulcehre, Dzmitry Bahdanau, Fethi Bougares, Holger Schwenk, and Yoshua Bengio. 2014. [Learning phrase representations using RNN encoder–decoder for statistical machine translation](#). In *Proceedings of the 2014 Conference on Empirical Methods in Natural Language Processing*, pages 1724–1734, Doha, Qatar.
- Ronan Collobert, Jason Weston, Léon Bottou, Michael Karlen, Koray Kavukcuoglu, and Pavel Kuksa. 2011. [Natural language processing \(almost\) from scratch](#). *Journal of Machine Learning Research*, 12:2493–2537.
- Yann N. Dauphin, Gökhan Tür, Dilek Hakkani-Tür, and Larry P. Heck. 2014. [Zero-shot learning and clustering for semantic utterance classification](#). In *International Conference on Learning Representations*, Banff, Canada.
- Orhan Firat, Baskaran Sankaran, Yaser Al-Onaizan, Fatos T. Yarman Vural, and Kyunghyun Cho. 2016. [Zero-resource translation with multi-lingual neural machine translation](#). In *Proceedings of the 2016 Conference on Empirical Methods in Natural Language Processing*, pages 268–277, Austin, USA.
- Andrea Frome, Greg S. Corrado, Jon Shlens, Samy Bengio, Jeff Dean, Marc Aurelio Ranzato, and Tomas Mikolov. 2013. [DeViSE: A deep visual-semantic embedding model](#). In C. J. C. Burges, L. Bottou, M. Welling, Z. Ghahramani, and K. Q. Weinberger, editors, *Advances in Neural Information Processing Systems 26*, pages 2121–2129. Curran Associates, Inc.
- Yanwei Fu, Tao Xiang, Yu-Gang Jiang, Xi-angyang Xue, Leonid Sigal, and Shaogang Gong. 2018. [Recent advances in zero-shot recognition: Toward data-efficient understanding of visual content](#). *IEEE Signal Processing Magazine*, 35(1):112–125.
- Rie Johnson and Tong Zhang. 2015. [Effective use of word order for text categorization with convolutional neural networks](#). In *Proceedings of the 2015 Conference of the North American Chapter of the Association for Computational Linguistics: Human Language Technologies*, pages 103–112, Denver, Colorado.
- Yoon Kim. 2014. [Convolutional neural networks for sentence classification](#). In *Proceedings of the 2014 Conference on Empirical Methods in Natural Language Processing*, pages 1746–1751, Doha, Qatar.
- Alexandre Klementiev, Ivan Titov, and Binod Bhattarai. 2012. [Inducing crosslingual distributed representations of words](#). In *Proceedings of COLING 2012*, pages 1459–1474, Mumbai, India.
- Ankit Kumar, Ozan Irsoy, Jonathan Su, James Bradbury, Robert English, Brian Pierce, Peter Ondruska, Ishaan Gulrajani, and Richard Socher. 2015. [Ask me anything: Dynamic memory networks for natural language processing](#). In *Proceedings of The 33rd International Conference on Machine Learning*, pages 334–343, New York City, USA.
- Siwei Lai, Liheng Xu, Kang Liu, and Jun Zhao. 2015. [Recurrent convolutional neural networks for text classification](#). In *Proceedings of the 29th AAAI Conference on Artificial Intelligence*, pages 2267–2273, Austin, USA.
- Quoc V. Le and Tomas Mikolov. 2014. [Distributed representations of sentences and documents](#). In *Proceedings of The 31st International Conference on Machine Learning*, pages 1188–1196, Beijing, China.
- Yann LeCun, Sumit Chopra, Raia Hadsell, Fu Jie Huang, and et al. 2006. [A tutorial on energy-based learning](#). In *Predicting Structured Data*. MIT Press.
- Jason Lee, Kyunghyun Cho, and Thomas Hofmann. 2017. [Fully character-level neural machine translation without explicit segmentation](#). *Transactions of the Association for Computational Linguistics*, 5:365–378.
- Rui Lin, Shujie Liu, Muyun Yang, Mu Li, Ming Zhou, and Sheng Li. 2015. [Hierarchical recurrent neural network for document modeling](#). In *Proceedings of the 2015 Conference on Empirical Methods in Natural Language Processing*, pages 899–907, Lisbon, Portugal.
- Thang Luong, Hieu Pham, and Christopher D. Manning. 2015. [Effective approaches to attention-based neural machine translation](#). In

- Proceedings of the 2015 Conference on Empirical Methods in Natural Language Processing*, pages 1412–1421, Lisbon, Portugal.
- Thomas Mensink, Jakob Verbeek, Florent Perronnin, and Gabriela Csurka. 2012. Metric learning for large scale image classification: Generalizing to new classes at near-zero cost. In *Computer Vision – ECCV 2012*, pages 488–501, Berlin, Heidelberg. Springer Berlin Heidelberg.
- Tomas Mikolov, Ilya Sutskever, Kai Chen, Greg S Corrado, and Jeff Dean. 2013. [Distributed representations of words and phrases and their compositionality](#). In C. J. C. Burges, L. Bottou, M. Welling, Z. Ghahramani, and K. Q. Weinberger, editors, *Advances in Neural Information Processing Systems 26*, pages 3111–3119. Curran Associates, Inc.
- Frederic Morin and Yoshua Bengio. 2005. [Hierarchical probabilistic neural network language model](#). In *Proceedings of the Tenth International Workshop on Artificial Intelligence and Statistics*, pages 246–252.
- Khalil Mrini, Nikolaos Pappas, and Andrei Popescu-Belis. 2017. [Cross-lingual transfer for news article labeling: Benchmarking statistical and neural models](#). In *Idiap Research Report*, Idiap-RR-26-2017.
- Junseok Nam, Eneldo Loza Mencía, and Johannes Fürnkranz. 2016. [All-in text: Learning document, label, and word representations jointly](#). In *Proceedings of the 13th AAI Conference on Artificial Intelligence*, AAI’16, pages 1948–1954, Phoenix, Arizona.
- Mohammad Norouzi, Tomas Mikolov, Samy Bengio, Yoram Singer, Jonathon Shlens, Andrea Frome, Greg Corrado, and Jeffrey Dean. 2014. [Zero-shot learning by convex combination of semantic embeddings](#). In *International Conference on Learning Representations*, Banff, Canada.
- Bo Pang and Lillian Lee. 2005. [Seeing stars: Exploiting class relationships for sentiment categorization with respect to rating scales](#). In *Proceedings of the 43rd Annual Meeting on Association for Computational Linguistics*, pages 115–124, Ann Arbor, Michigan.
- Nikolaos Pappas, Lesly Miculicich, and James Henderson. 2018. [Beyond weight tying: Learning joint input-output embeddings for neural machine translation](#). In *Proceedings of the Third Conference on Machine Translation: Research Papers*, pages 73–83, Belgium, Brussels. Association for Computational Linguistics.
- Nikolaos Pappas and Andrei Popescu-Belis. 2017. [Multilingual hierarchical attention networks for document classification](#). In *Proceedings of the Eighth International Joint Conference on Natural Language Processing (Volume 1: Long Papers)*, pages 1015–1025.
- Alexander M. Rush, Sumit Chopra, and Jason Weston. 2015. [A neural attention model for abstractive sentence summarization](#). In *Proceedings of the 2015 Conference on Empirical Methods in Natural Language Processing*, pages 379–389, Lisbon, Portugal.
- Rico Sennrich, Barry Haddow, and Alexandra Birch. 2016. [Neural machine translation of rare words with subword units](#). In *Proceedings of the 54th Annual Meeting of the Association for Computational Linguistics (Volume 1: Long Papers)*, pages 1715–1725, Berlin, Germany.
- Lei Shu, Hu Xu, and Bing Liu. 2017. [DOC: Deep open classification of text documents](#). In *Proceedings of the 2017 Conference on Empirical Methods in Natural Language Processing*, pages 2911–2916, Copenhagen, Denmark. Association for Computational Linguistics.
- Richard Socher, Milind Ganjoo, Christopher D. Manning, and Andrew Y. Ng. 2013. [Zero-shot learning through cross-modal transfer](#). In *Proceedings of the 26th International Conference on Neural Information Processing Systems*, NIPS’13, pages 935–943, Lake Tahoe, Nevada.
- Vivek Srikumar and Christopher D. Manning. 2014. [Learning distributed representations for structured output prediction](#). In *Proceedings of the 27th International Conference on Neural Information Processing Systems - Volume 2*, NIPS’14, pages 3266–3274, Cambridge, MA, USA. MIT Press.
- Duyu Tang, Bing Qin, and Ting Liu. 2015. [Document modeling with gated recurrent neural](#)

- network for sentiment classification. In *Proceedings of the 2015 Conference on Empirical Methods in Natural Language Processing*, pages 1422–1432, Lisbon, Portugal. Association for Computational Linguistics.
- Guoyin Wang, Chunyuan Li, Wenlin Wang, Yizhe Zhang, Dinghan Shen, Xinyuan Zhang, Ricardo Henao, and Lawrence Carin. 2018. [Joint embedding of words and labels for text classification](#). In *Proceedings of the 56th Annual Meeting of the Association for Computational Linguistics (Volume 1: Long Papers)*, pages 2321–2331. Association for Computational Linguistics.
- Jason Weston, Samy Bengio, and Nicolas Usunier. 2010. [Large scale image annotation: Learning to rank with joint word-image embeddings](#). *Mach. Learn.*, 81(1):21–35.
- Jason Weston, Samy Bengio, and Nicolas Usunier. 2011. [WSABIE: Scaling up to large vocabulary image annotation](#). In *Proceedings of the Twenty-Second International Joint Conference on Artificial Intelligence (Volume 3)*, pages 2764–2770, Barcelona, Spain.
- Zichao Yang, Diyi Yang, Chris Dyer, Xiaodong He, Alex Smola, and Eduard Hovy. 2016. [Hierarchical attention networks for document classification](#). In *Proceedings of the 2016 Conference of the North American Chapter of the Association for Computational Linguistics: Human Language Technologies*, pages 1480–1489, San Diego, California.
- Majid Yazdani and James Henderson. 2015. [A model of zero-shot learning of spoken language understanding](#). In *Proceedings of the 2015 Conference on Empirical Methods in Natural Language Processing*, pages 244–249, Lisbon, Portugal.
- Chih-Kuan Yeh, Wei-Chieh Wu, Wei-Jen Ko, and Yu-Chiang Frank Wang. 2018. [Learning deep latent spaces for multi-label classification](#). In *Proceedings of the 32nd AAAI Conference on Artificial Intelligence*, New Orleans, USA.
- Xiang Zhang, Junbo Zhao, and Yann LeCun. 2015. [Character-level convolutional networks for text classification](#). In *Advances in Neural Information Processing Systems 28*, pages 649–657, Montreal, Canada.
- Yang Zhang, Boqing Gong, and Mubarak Shah. 2016. [Fast zero-shot image tagging](#). In *Proceedings of the IEEE Conference on Computer Vision and Pattern Recognition*, Las Vegas, USA.